Poly(ethylene oxide)/poly(methyl methacrylate) blends: Influence of tacticity of poly(methyl methacrylate) on blend structure and miscibility

C. Silvestre, S. Cimmino and E. Martuscelli
Istituto di Ricerche su Tecnologia dei Polimeri e Reologia, CNR Arco Felice, Napoli, Italy

and F. E. Karasz and W. J. MacKnight
Polymer Science and Engineering Department, University of Massachusetts, Amherst, Mass, USA
(Received 22 July 1986; revised 27 October 1986; accepted 12 November 1986)

The influence of different configurations of poly(methyl methacrylate) on the miscibility and superstructure of poly(ethylene oxide)/poly(methyl methacrylate) (PEO/PMMA) blends was examined using small-angle X-ray scattering and differential scanning calorimetry. The blends prepared by solution casting were isothermally crystallized at 48°C. The miscibility, the melting behaviour, the glass transition temperature and the structural parameters of the blends were strongly dependent on the tacticity and blend composition. The small-angle X-ray intensity profiles were analysed using a recently developed methodology. For the poly(ethylene oxide)/atactic poly(methyl methacrylate) (PEO/APMMA) and poly(ethylene oxide)/syndiotactic poly(methyl methacrylate) (PEO/SPMMA) blends, the long period and the amorphous and transition region thicknesses increased with increase of PMMA content, whereas for the poly(ethylene oxide)/isotactic poly(methyl methacrylate) (PEO/IPMMA) blends they are independent of composition. The structural properties of the blends were attributed to the presence of non-crystallizable material in the interlamellar or interfibrillar regions, depending on PMMA tacticity. From the glass transition and melting temperatures, it has been supposed that one homogeneous amorphous phase is present in the case of PEO/APMMA and PEO/SPMMA blends and that the PEO/IPMMA amorphous system is phase-separated. The free-volume contribution to the energy of mixing for the various tactic PMMAs is hypothesized to be responsible for the difference in mixing behaviour.

INTRODUCTION

A number of papers have recently shown that the tacticity of poly(methyl methacrylate) (PMMA) influences blend compatibility, when PMMA with different configurations is blended with a chemically different polymer[1-4]. According to recent theories of polymer mixing[5-12], the free energy of mixing consists of three main contributions: the combinatorial entropy of mixing, the exchange interaction and the free-volume contribution. For high molar mass components, all three contributions are very small and the observed phase behaviour is the result of a very delicate balance among them. Theoretically, a change in tacticity of a blend component may lead to a change in the free-volume contribution. Moreover, the influence of conformation and radius of gyration of the various tactic forms on the total number and strength of the exchange interactions must be taken into account for the energy balance.

Schurer *et al.*[1], studying blends of poly(vinyl chloride) (PVC) and PMMA concluded through detection of one or two T_g values that PVC was partially miscible with atactic (A) and syndiotactic (S) PMMA, but almost completely immiscible with isotactic (I) PMMA. On the same system, more recently Vorenkamp *et al.*[4] made a more quantitative statement about the influence of the tacticity of PMMA on its miscibility with PVC. In fact, using Flory's equation-of-state theory, it was possible to attribute the difference in phase behaviour between the PVC/SPMMA and the PVC/IPMMA blends to the free-volume contribution to the energy of mixing.

The occurrence of a single glass transition temperature over a broad composition range, as well as lowering of the crystallization and melting temperatures, indicated complete miscibility of poly(vinylidene fluoride) (PVF_2) with IPMMA, APMMA and SPMMA[2,3]; on the other hand, the lowest value of interaction parameter for the PVF_2/IPMMA system, obtained by applying the Nishi and Wang[13] equation to the equilibrium melting point depression, seems to indicate that the interaction of PVF_2 segments with IPMMA segments is stronger than with APMMA and SPMMA segments. In this paper the influence of tacticity of PMMA on the phase structure, compatibility and superstructure of poly(ethylene oxide)(PEO)/PMMA blends has been studied, using small-angle X-ray scattering (SAXS) and differential scanning calorimetry (d.s.c.).

0032-3861/87/071190-10$03.00

Blends of PEO and APMMA are among the most studied polymer systems, consisting of a crystallizable component and an amorphous one[14-25]. The depression of the equilibrium melting temperature and of the spherulite radial growth rate[15,16,19,20,22], the composition dependence of ^{13}C dynamic parameters of the PEO[17] and the presence of a single glass transition temperature lead to the conclusion that PEO and APMMA are compatible in the amorphous state. Also a theoretical approach[14], using the solubility parameters, has underlined that PEO and APMMA form compatible mixtures for temperatures higher than 55°C. Using vibrational spectroscopy[26] it has been shown that upon blending the PEO preferentially takes a planar zig-zag structure and that the compatibility is due to van der Waals type bonding between planar PEO segments and APMMA ones. In the same paper, on the basis of the molecular models it was predicted that the PEO/IPMMA blend would be more miscible than the PEO/SPMMA one.

The principal aim of this work is to study the extent of mixing of the PEO and PMMA in the amorphous phase depending on PMMA tacticity and blend composition by using small-angle X-ray scattering and differential scanning calorimetry. These techniques have been shown to be valuable tools to obtain information on the macrostructural parameters and phase behaviour of blends containing a semicrystallizable polymer and an amorphous one[27-32].

EXPERIMENTAL

Materials and blend preparation

The molecular characteristics together with the glass transition temperatures of the polymers used in this study are reported in *Table 1*. The binary blends were prepared by casting a 10% (w/v) solution of a preweighed mixture of PEO and PMMA in chloroform onto flat Petri dishes at room temperature. To ensure complete removal of the solvent the resulting powders were kept under vacuum at 70°C for 24 h. The pure PEO and the 90/10, 80/20, 70/30 and 60/40 PEO/PMMA blends containing all the various tactic forms of PMMA were investigated.

The dried blends and the pure PEO were compression moulded at 1000 psi and 70°C with the aid of a Carver press. The mould containing the sample was sealed in aluminium foil and kept in a bath set at 80°C for 10 min, to allow the melting of the sample. Then it was rapidly transferred to the crystallization bath set at 48°C and kept at this temperature for 3 days to ensure complete crystallization.

SAXS analysis

SAXS studies were carried out using a Kratky camera assuming infinite slit-height geometry. To produce X-rays, a Kratky Siemens Ag 40/copper target X-ray tube in connection with a Philips Norelco generator operating at 40 kV and 20 mA was used. Detection was done by employing a Braun one-dimensional position-sensitive detector. The raw scattering data were corrected for the sensitivity of the detector, electron noise and parasitic scattering. The parasitic scattering intensity multiplied by the sample attenuation coefficient was subtracted from the sample data set.

To perform quantitative analysis of the scattering arising from lamellar interference, the contribution to the scattering due to thermal density fluctuation within phases and to wide-angle scattering (background scattering) must first be removed. In this study the background scattering was assumed constant with respect to the scattering vector **s**, whose magnitude is $s=(2/\lambda)\sin\theta$, where λ is the wavelength of the incident radiation and 2θ is the angle between the incident radiation direction and the observer. Finally in some cases desmearing of the scattering curves was performed, according to Vonk, using the measured slit intensity profile[33]. The desmeared intensities were Lorentz factor corrected[34], multiplying them by s^2. Guinier has shown that the scattered intensity $I(s)$ for an isotropic system can be represented by the following relation[35,36]:

$$I(s)=\frac{i_e I_0}{p^2}\overline{\eta^2}V_0\int_0^\infty \gamma(r)\exp(2\pi isr)\mathrm{d}r \qquad (1)$$

where i_e is the Thompson scattering factor, I_0 the incident intensity of X-rays, p the distance from the scattering material to the detector, V_0 the volume of the scattering system, and $\gamma(r)$ the three-dimensional correlation function.

The three-dimensional correlation function can be described as

$$\gamma(r)=\frac{\langle \Delta\eta_j \Delta\eta_k\rangle_r}{\overline{\eta^2}} \qquad (2)$$

where $\Delta\eta_i$ is the deviation of the electron density of the ith volume element from the average, $\langle\ \ \rangle_r$ represents the average fluctuation over all volume elements separated by a distance r and $\overline{\eta^2}$ is the mean square fluctuation at $r=0$.

A Fourier transform of (1) enables one to solve $\gamma(r)$ in terms of $I(s)$ obtaining

$$\gamma(r)=\frac{\int_0^\infty I(s)\cos(2\pi rs)\mathrm{d}s}{\int_0^\infty I(s)\mathrm{d}s} \qquad (3)$$

Table 1 Characteristics of the materials used

Polymer	$\bar{M}_w\times10^{-3}$ [a]	$\bar{M}_n\times10^{-3}$ [a]	T_g (°C)[b]
Poly(ethylene oxide), PEO	20	–	−65
Syndiotactic poly(methyl methacrylate), SPMMA	319	155	127
Atactic poly(methyl methacrylate), APMMA	–	116	115
Isotactic poly(methyl methacrylate), IPMMA	132	26	60

[a] Molecular weights obtained by g.p.c. measurements
[b] Glass transition temperatures obtained by d.s.c. measurements

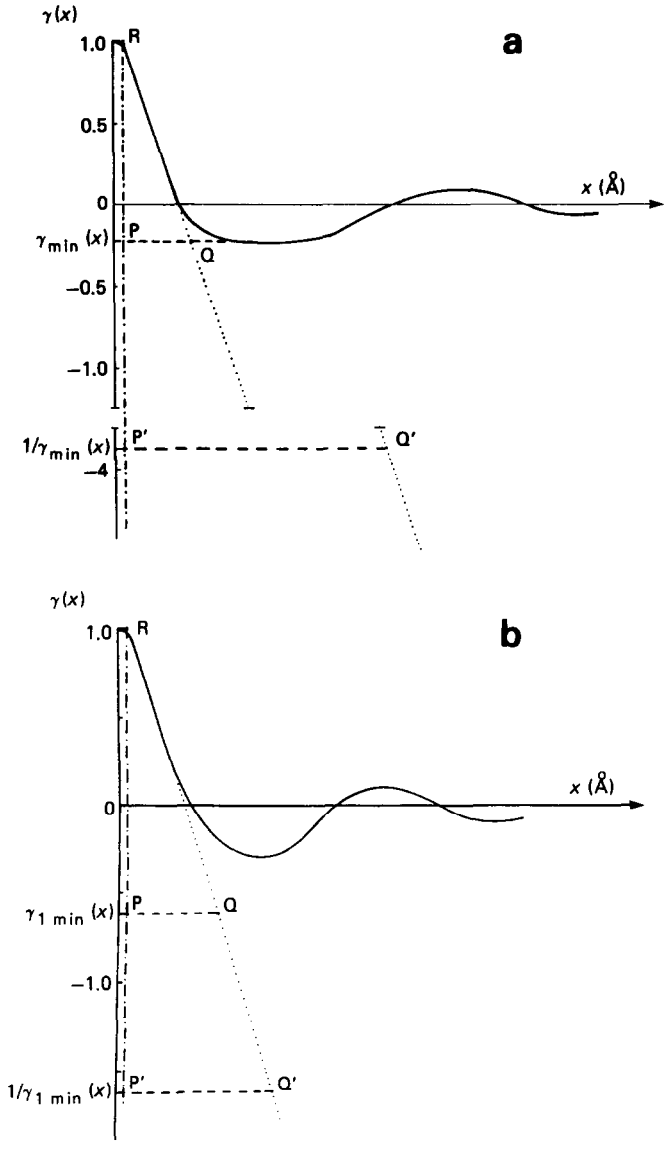

Figure 1 One-dimensional correlation function $\gamma(x)$ (full curve) *versus* correlation distance x. (a) General features: R is the intersection point between the extrapolation (dotted line) of the stright line beyond the curvature of $\gamma(x)$ at the origin and the horizontal line at $\gamma(x)=1$; the position of R is at $x=E/3$; P and P' are the intersection points between the vertical line (chain line) at $x=$OR and the horizontal lines (broken lines) at $\gamma(x)=\gamma_{min}(x)$ and $\gamma(x)=1/\gamma_{min}(x)$ respectively; Q and Q' are the intersection points between the dotted lines and the broken lines. (b) Features of the one-dimensional correlation function when there is no plateau in the region of the first minimum: $\gamma_{min}(x)$ is the theoretical value of the minimum in the one-dimensional correlation function, obtained from equations (5) and (6) by using the d.s.c. crystallinity instead of ϕ_s

The scattering intensity, experimentally determined, is from a three-dimensional system and must be corrected to compare with scattering calculated for models containing one-dimensional lamellar structure. This is accomplished by multiplying the $I(s)$ by s^2 (Lorentz correction).

The expression for the one-dimensional correlation function is

$$\gamma(x)=\frac{\int_0^\infty I(s)s^2\cos(2\pi xs)\mathrm{d}s}{\int_0^\infty s^2 I(s)\mathrm{d}s} \tag{4}$$

The general features of the one-dimensional correlation function as obtained from (4) are shown in *Figure 1a*. The first maximum corresponds to the average value of the distance of periodicity. The width of the phase boundary, E, is reflected in the curvature of $\gamma(x)$ at the origin. It can be shown that segment OR$=E/3$ if the variation of the electron density in the transition layer is linear (see *Figure 2*).

According to Vonk and Korleve[37] if $\gamma(x)$ shows a plateau in the region of the first minimum, this can be related to the volume fraction crystallinity, ϕ_s, using the expression:

$$\gamma_{min}^{(x)}=-\frac{1-\phi_s}{\phi_s} \tag{5}$$

or

$$\gamma_{min}^{(x)}=-\frac{\phi_s}{1-\phi_s} \tag{6}$$

where (5) applies when $\phi_s>0.5$, and (6) when $\phi_s<0.5$.

The slope of the linear region in $\gamma(x)$ beyond the curvature at the origin and the lines section PQ and P'Q', at levels $\gamma(x)=\gamma_{min}^{(x)}$ and $\gamma(x)=1/\gamma_{min}^{(x)}$ respectively, can be used to find the amorphous and crystalline layers ($\langle t_s\rangle_n$ and $\langle t_c\rangle_n$) with the aid of the relations

$$\mathrm{PQ}=\langle t_a\rangle_n-\frac{\langle E\rangle_n}{3(1-\phi_s)} \tag{7a}$$

$$\mathrm{P'Q'}=\langle t_c\rangle_n-\frac{\langle E\rangle_n}{3\phi_s} \tag{7b}$$

These relations are valid only in the case of one-dimensional structure with alternating parallel crystalline and amorphous lamellae and for $\phi_s>0.5$. The average crystalline thickness $\langle C\rangle_n$ and the average amorphous thickness $\langle A\rangle_n$ can now be easily obtained using the relations

$$\langle C\rangle_n=\langle t_c\rangle_n-\langle E\rangle_n \tag{8}$$

$$\langle A\rangle_n=\langle t_a\rangle_n-\langle E\rangle_n \tag{9}$$

Very often in experimental practice, as reported by Vonk[37], the $\gamma(x)$ does not show a plateau in the region of the first minimum (see *Figure 1b*), because the wings of the first maximum can cover part of the minimum. Therefore the experimental value of $\gamma_{min}^{(x)}$ is higher than the real one

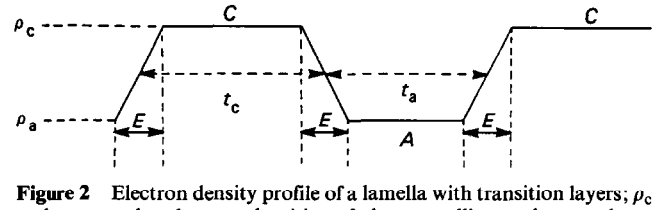

Figure 2 Electron density profile of a lamella with transition layers; ρ_c and ρ_a are the electron densities of the crystalline and amorphous phases, respectively; t_c and t_a are the total thicknesses of the crystalline and amorphous layers, respectively, and they pertain to the midplane of the transition layer; C is the thickness of the crystalline lamella, attaining the maximum value of the electron density; A is the thickness of the amorphous region, attaining the minimum value of the electron density; E is the transition layer thickness

and cannot be used in order to obtain ϕ_s (equations (5) and (6)), PQ and P'Q' and hence to calculate $\langle t_a \rangle_n$ and $\langle t_c \rangle_n$ (equations (7)).

As we already did in a previous paper[27] this obstacle can be overcome using in (5), (6) and (7) the crystallinity by d.s.c. instead of ϕ_s. In this way a new value of the minimum in the one-dimensional correlation function, $\gamma^{(x)}_{1\min}$, is found, which can be used in order to get the crystalline and amorphous lamellar thickness.

The model used in this work to describe the scattering from a lamellar structure is the lamellar pseudo-two-phase structure as discussed by Vonk[38]. A lamellar pseudo-two-phase structure is defined as consisting of alternating parallel crystalline and amorphous lamellae, connected by transition layers, which are placed in stacks that are large enough not to affect the small-angle scattering. The profile of the electron density of the model is reported in *Figure 2*. According to this model the density gradient differs from zero only in the transition layer, where the density varies linearly between the values of the electron densities of the crystalline and amorphous layers.

Calorimetric measurements

The index of crystallinity, the glass transition temperatures and the melting temperatures of pure PEO and of blends crystallized isothermally were obtained using a differential scanning calorimeter. The apparent enthalpies of fusion and the melting temperatures were derived respectively from the area and the maximum of the d.s.c. endotherm peaks. A scanning rate of 10°C min^{-1} was always used.

The weight crystallinity indexes of the PEO phase, X_c(PEO), and of the overall blends, X_c(blend), were calculated from

$$X_c(\text{PEO}) = \frac{\Delta H^*(\text{PEO})}{\Delta H^\circ(\text{PEO})} \qquad X_c(\text{blend}) = \frac{\Delta H^*(\text{blend})}{\Delta H^\circ(\text{PEO})} \qquad (10)$$

where ΔH°(PEO) is the heat of melting per gram of 100% crystalline PEO (from literature data[39] $\Delta H^\circ(\text{PEO}) = 49$ cal g^{-1}, ΔH^*(PEO) and ΔH^*(blend) are the apparent enthalpies of melting per gram of PEO in the blend and for a gram of blend respectively.

In order to determine the glass transition temperature the isothermally crystallized sample was heated from −100 to 150°C and the heat evolved was recorded as a function of the temperature. The T_g of the samples was taken as the temperature corresponding to 50% of the transition.

RESULTS AND DISCUSSION

Melting temperature and crystallinity index

The melting temperatures, T_m, as functions of composition for all the blends crystallized at $T_c = 48$°C are reported in *Table 2*. For the blends containing APMMA and IPMMA, T_m is almost constant with composition. In the case of PEO/SPMMA it decreases monotonically with increase of SPMMA. In general a decrease in the melting point in a polymeric blend can be due both to morphological effects (decrease in lamellar thickness) and to thermodynamic factors (polymer–polymer interactions)[40,41]. As will be shown by SAXS analysis (see next section) the lamellar thickness for PEO/SPMMA blends is independent of composition. Therefore the decrease in T_m cannot be attributed to such a morphological effect, and even if we are not considering the equilibrium melting point, it can suggest that favourable interactions can occur between the two components (diluent effect). Studies are in progress on this subject.

The crystallinity indices of the blends, X_c(blend), and of the PEO phase, X_c(PEO), are reported in *Table 3*. The X_c(blend) and X_c(PEO) values are dependent on tacticity and composition. The X_c(blend) decreases almost monotonically with composition for all the blends and, at a given composition, such a decrease is more marked for blends containing SPMMA. The X_c(PEO) for the PEO/APMMA blends remains almost constant with composition up to 20% of PMMA, whereas for blends with higher PMMA content it is possible to note a decrease in the crystallinity values. In the case of PEO/SPMMA, X_c(PEO) decreases with increase of the amorphous material, whereas it seems to be higher than that corresponding to pure PEO for the blends containing IPMMA. These results can indicate that the PEO is not allowed to crystallize completely and/or perfectly when it is blended with syndiotactic and with atactic PMMA at concentrations higher than 20%, whereas the addition of IPMMA to PEO seems to lead to more complete crystallization of the poly(ethylene oxide).

This behaviour may be explained by the different mobilities of the crystallizable chains in the melt depending on the different PMMA used. In fact, due to the different values of T_g of the PMMAs (see *Table 1*), the melt viscosity of the material surrounding the PEO

Table 2 Melting temperature, T_m (°C)

Blend composition, PEO/PMMA (wt/wt)	T_m (°C)[a]		
	PEO/APMMA	PEO/IPMMA	PEO/SPMMA
100/0	69	69	69
90/10	69	69	68
80/20	69	70	69
70/30	68	68	66
60/40	68	68	65

[a] Error ±1°C

Table 3 Overall crystallinity index, X_c(blend) (%), and crystallinity index of the PEO phase, X_c(PEO) (%)

Blend composition, PEO/PMMA (wt/wt)	X_c(blend) (%)[a]		
	PEO/APMMA	PEO/IPMMA	PEO/SPMMA
100/0	90	90	90
90/10	80	82	78
80/20	71	75	69
70/30	60	64	54
60/40	50	55	43
Blend composition, PEO/PMMA (wt/wt)	X_c(PEO) (%)[a]		
	PEO/APMMA	PEO/IPMMA	PEO/SPMMA
100/0	90	90	90
90/10	89	91	87
80/20	89	94	86
70/30	86	91	77
60/40	83	92	72

[a] Error ±2%

Table 4 Composition of the amorphous phase in PEO/PMMA blends and relative glass transition temperature, T_g (°C)

Nominal blend composition, PEO/PMMA (wt/wt)	Composition of amorphous phase in PEO/PMMA blends (wt/wt)			T_g (°C) relative to amorphous phase of PEO/PMMA blends, calculated by Fox equation		
	PEO/APMMA	PEO/IPMMA	PEO/SPMMA	PEO/APMMA	PEO/IPMMA	PEO/SPMMA
100/0	100/0	100/0	100/0	−65	−65	−65
90/10	50/50	45/55	52/48	−2	−11	−2
80/20	31/69	19/81	46/54	34	26	27
70/30	25/75	17/83	35/65	47	29	30
60/40	20/80	11/89	30/70	58	39	41

crystallites is much lower for the PEO/IPMMA system than for the PEO/APMMA and PEO/SPMMA ones. Therefore the rate of diffusion of chain segments and hence the rate of crystallization and reorganization is higher for the PEO/IPMMA blend, giving PEO the possibility to crystallize in a more complete way.

Glass transition temperatures

Generally in the literature, based on the behaviour of the glass transition and morphological evidence, the PEO/APMMA blend is reported to be miscible at all compositions above the melting point of the PEO[20,24,26]. Several authors have studied the miscibility of this system using d.s.c. Li and Hsu[24] have reported that, when molten blends were quenched directly in the d.s.c. instrument, a single glass transition temperature was observed in all cases. The values fitted the Fox equation[42] curve with some deviation for samples at high PEO content. The same authors have also reported that blends containing PEO with concentration equal to and less than 50%, crystallized up to 30 days at room temperature, presented two glass transitions. Liberman *et al.*[26] paid particular attention to blends containing PEO up to 20%. The thermograms revealed the presence of one single T_g, whose values decreased as the PEO content increased in the blend.

In this section we report the analysis of T_g measurements for the PEO/APMMA, PEO/APMMA and PEO/SPMMA blends with high PEO concentration, down to 60%. Our aim is to ascertain the influence of tacticity of PMMA on the miscibility of PEO/PMMA blends.

The glass transitions of a polymeric crystalline blend are related only to the amorphous material of the blend components. The composition of the amorphous PEO/PMMA blends used in this study, corrected for the PEO crystallinity, are reported in *Table 4*. In the same table we also report the values of the corresponding T_g, obtained by using the Fox equation[42]:

$$1/T_g = W_1/T_{g1} + W_2/T_{g2} \qquad (11)$$

In (11), W_1 and T_{g1}, and W_2 and T_{g2} are the weight fraction and the glass transition temperature of plain PEO and PMMA, respectively. This equation assumes miscibility at a random level. For all the systems studied, the T_g values predicted by the Fox equation are very close and sometimes included in the PEO melting temperature range (20–90°C). If the PEO/PMMA blends followed equation (11) T_g would be masked by the endotherm peak and consequently would not be detected in the d.s.c. thermogram.

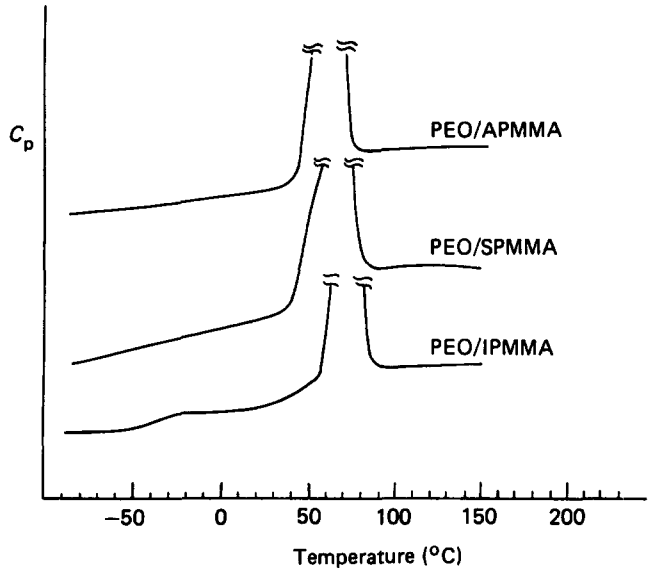

Figure 3 D.s.c. thermograms of 60/40 PEO/PMMA mixtures

The values of T_g of pure polymers are reported in *Table 1*. Typical thermograms of the PEO/APMMA, PEO/SPMMA and PEO/IPMMA blends, crystallized isothermally at 48°C, are shown in *Figure 3*. For the sake of clarity, we report only results for the 60/40 blends, because for a given PMMA tactic form, all the systems behaved in the same way independently of the blend composition. From the experimental results we are not able to carry out a quantitative analysis, just a qualitative one.

On the thermograms of PEO/APMMA and PEO/SPMMA blends there is no evidence of a T_g transition even when these traces are subjected to high magnification. This result can be accounted for if we assume that PEO/APMMA and PEO/SPMMA blends follow the Fox equation, i.e. they form a miscible blend in the molten state with a T_g transition masked by the PEO endothermic peak. The thermograms of PEO/IPMMA blends present a clear T_g always at about −40°C for all the compositions we have tested. The detection of one T_g for these blends at a temperature lower than that predicted by Fox seems to be evidence that the PEO/IPMMA system is separated into two phases, one rich in PEO and the other rich in IPMMA. The T_g for this second phase should be at higher temperature, close to the endotherm peak, and hence also in this case masked by it since the T_g of the pure IPMMA as measured by us is 60°C (see *Table 1*).

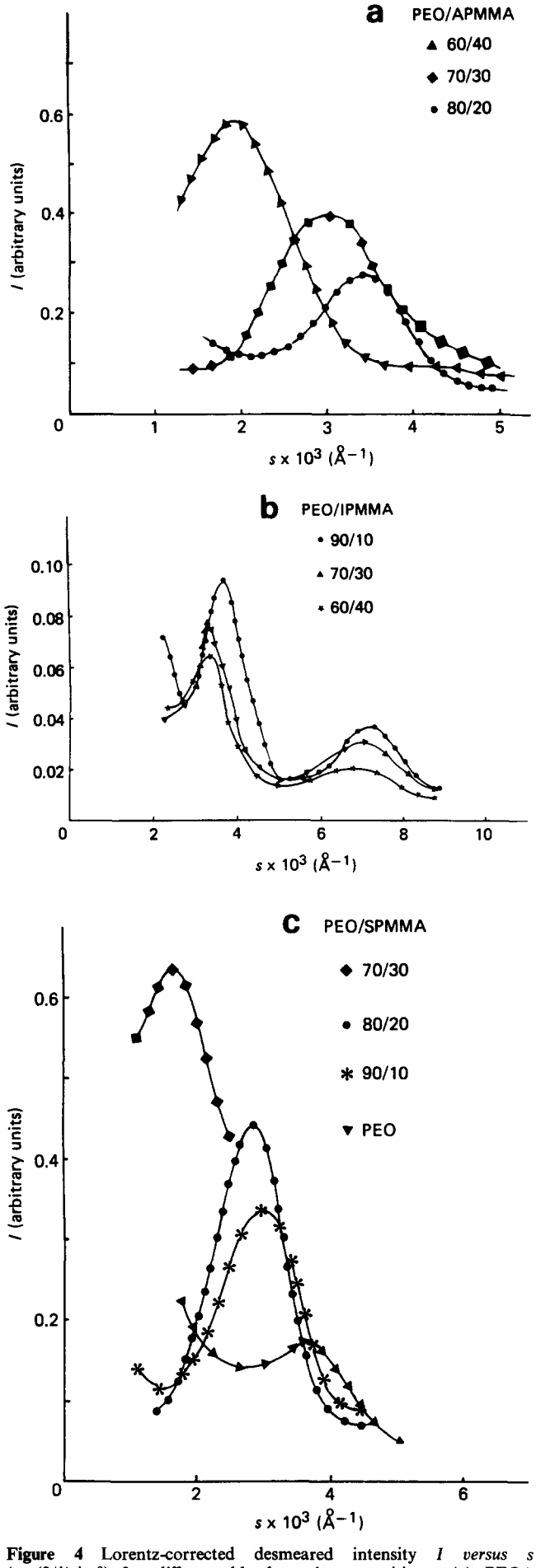

Figure 4 Lorentz-corrected desmeared intensity I *versus* s ($s=(2/\lambda)\sin\theta$) for different blends and compositions: (a) PEO/APMMA; (b) PEO/IPMMA; (c) PEO/SPMMA

SAXS investigation

The SAXS Lorentz-corrected desmeared patterns for the PEO/APMMA, PEO/IPMMA and PEO/SPMMA blends are presented in *Figure 4*. For the PEO/APMMA and PEO/SPMMA blends, the peak position shifts towards smaller s and the total scattering intensity increases as more PMMA is added to PEO. In the case of PEO/IPMMA blends, the peak position stays almost constant with composition and a decrease in the total scattered intensity is observed (see *Figure 4b*). For such a blend, two maxima can be observed. The ratio of the Lorentz-corrected scattering angle for the second maximum to that of the first is always close to a value of 2 and indicates that the second peak is a second-order maximum arising from the same structure. The presence of two peaks suggests that the addition of IPMMA to PEO may lead to an overall structure characterized by a more regular alternation of crystalline and amorphous regions. This is in agreement with the increase in crystallinity of the PEO phase observed for the same blends.

Using Bragg's law, the long periods, L, calculated from the peak position are obtained for all the samples. The values of L as functions of composition for all blends are plotted in *Figure 5*. As shown in this figure L increases exponentially with the content of APMMA and SPMMA, whereas for blends containing IPMMA L is almost independent of composition. Examples of the one-dimensional correlation function for the three blends are reported in *Figure 6*. The position of the first maximum in the one-dimensional correlation function is reported in *Table 5*. Good agreement with the values of the long period is seen. For the 60/40 and 70/30 PEO/SPMMA blends the correlation functions were so spread that no peak was observed.

For the PEO/SPMMA and PEO/APMMA blends no well defined horizontal region is observed in the first minimum of the one-dimensional correlation function (see *Figures 6a* and *6c*) and hence the experimental value of $\gamma_{min}(x)$ is higher than the real one. As we have already reported in the theoretical section, the crystallinity by d.s.c. was used to obtain a new value of $\gamma_{min}(x)$ and through this to calculate the values of $\langle A\rangle_n$ and $\langle C\rangle_n$ (see theoretical section).

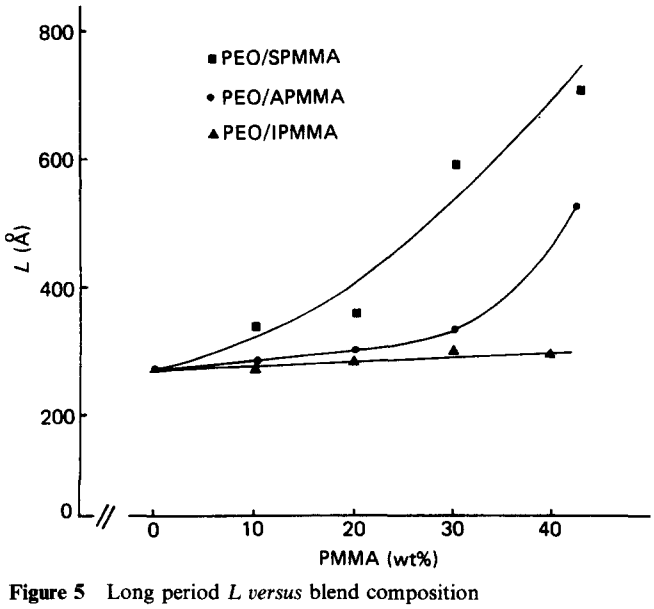

Figure 5 Long period L *versus* blend composition

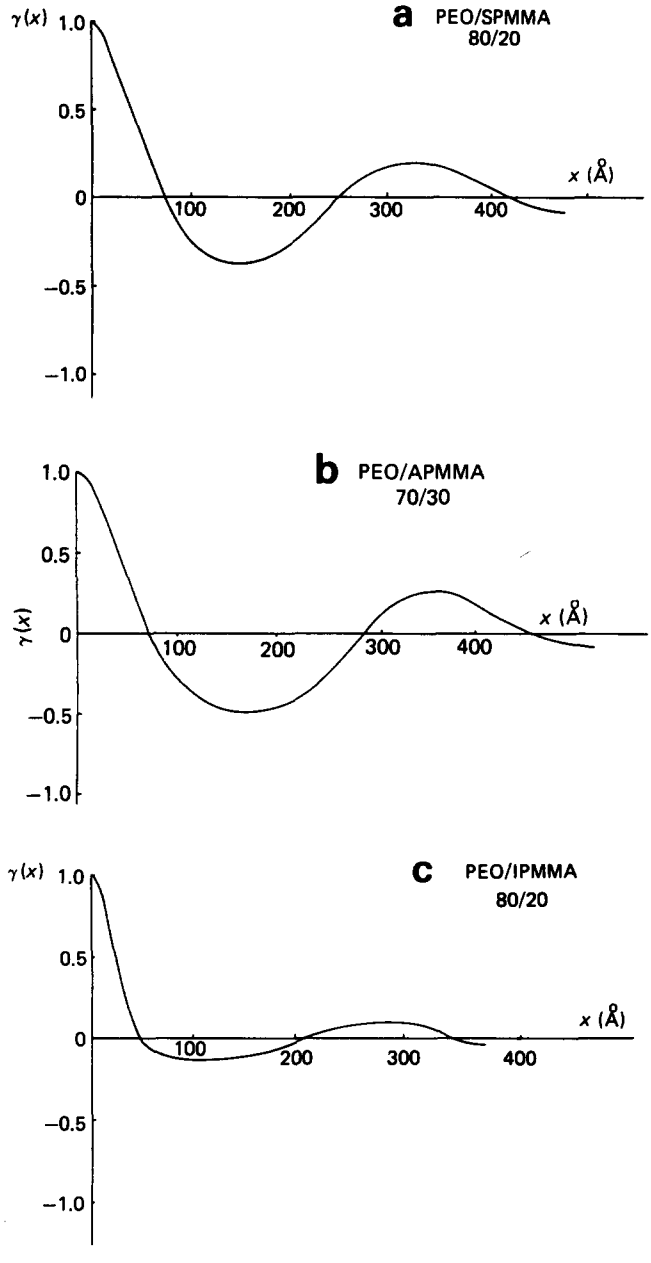

Figure 6 Examples of experimental one-dimensional correlation functions: (a) 80/20 wt% PEO/SPMMA blend; (b) 70/30 wt% PEO/APMMA blend; (c) 80/20 wt% PEO/IPMMA blend

Table 5 First peak position of the one-dimensional correlation function

Blend composition, PEO/PMMA (wt/wt)	First peak position (Å)[a]		
	PEO/APMMA	PEO/IPMMA	PEO/SPMMA
100/0	265	265	265
90/10	281	280	324
80/20	295	300	365
70/30	320	295	–
60/40	495	300	–

[a] Error ±10 Å

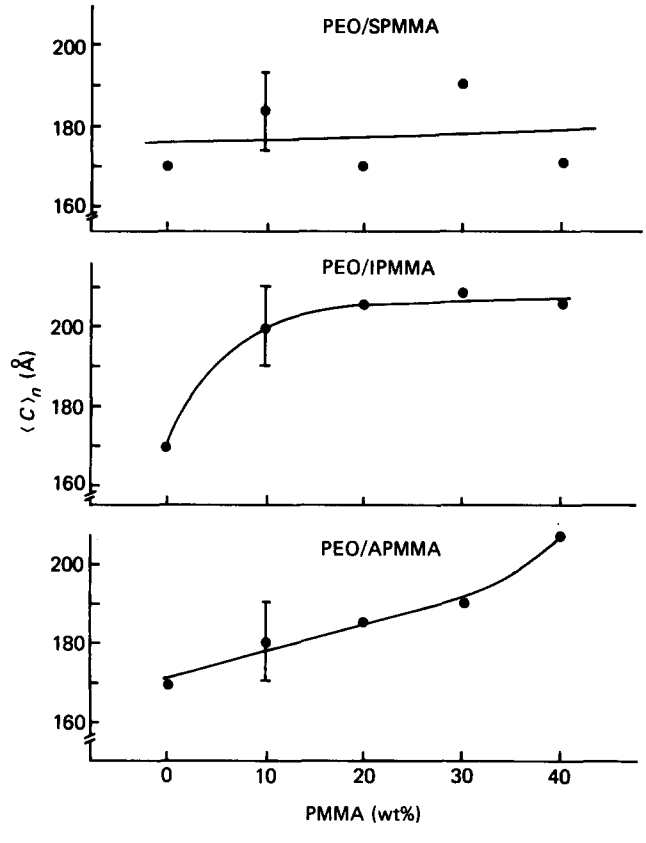

Figure 7 Average crystal thickness $\langle C \rangle_n$ *versus* blend composition

In the case of PEO/IPMMA blends a well defined horizontal region is present and from the value of $\gamma_{min}(x)$ the SAXS linear crystallinity is obtained, using relations (5) and (6). The SAXS crystallinities are in good agreement with the crystallinities referred to the PEO phase obtained by d.s.c. for these blends.

Using the relations described in the theoretical section the average size of the crystalline $\langle C \rangle_n$ and amorphous $\langle A \rangle_n$ regions and of the transition layer $\langle E \rangle_n$ are obtained. The results are reported in *Figures 7–9*. For the PEO/SPMMA blends the $\langle C \rangle_n$ values are within experimental errors of each other with no dependence on blend composition. In the case of PEO/APMMA blends $\langle C \rangle_n$ increases almost linearly with composition, whereas, for blends containing IPMMA, on adding 10% of PMMA to PEO we observe an abrupt increase in the $\langle C \rangle_n$ values, which on further addition of IPMMA remains constant. It should be noted that $\langle C \rangle_n$ for the PEO/IPMMA blend is always higher than the crystal

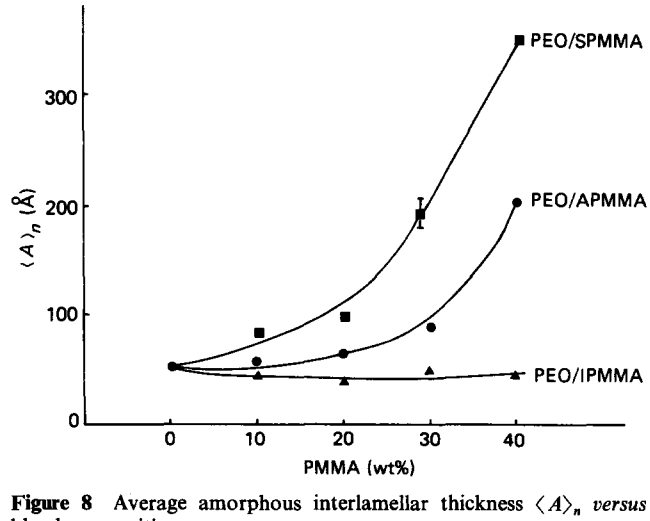

Figure 8 Average amorphous interlamellar thickness $\langle A \rangle_n$ *versus* blend composition

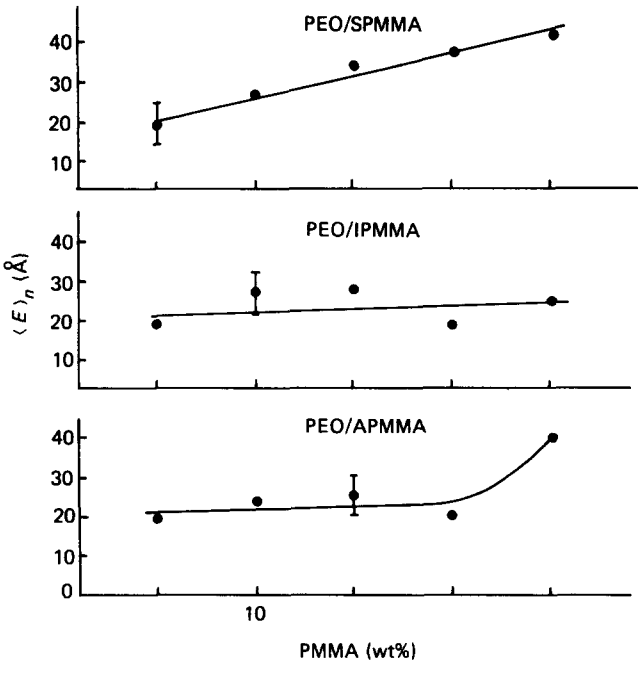

Figure 9 Average interphase thickness $\langle E \rangle_n$ *versus* blend composition

thickness of pure PEO and of PEO crystallized from PEO/SPMMA and PEO/APMMA blends.

On the basis of the kinetic theory of crystallization[43] the crystalline lamellar thickness is mainly dependent on the undercooling and at a given T_c on the rate of annealing. With the data at hand it is hard to explain the variation observed in the $\langle C \rangle_n$ values, which depend on tacticity and composition, and it remains a fascinating study that we are carrying on in our laboratory.

The transition and amorphous layer thicknesses $\langle E \rangle_n$ and $\langle A \rangle_n$ for the PEO/IPMMA blends are almost independent of composition; in the case of PEO/SPMMA they both increase with increasing SPMMA content in the blend. For the PEO/APMMA blends $\langle A \rangle_n$ increases with composition, whereas $\langle E \rangle_n$ remains constant up to blends containing 30 wt% of PMMA and increases for the 60/40 PEO/APMMA blend.

On the basis of the model used, the SAXS analysis, together with the preliminary microscopic observation that for any blends at any composition studied the PEO crystalline superstructures were volume filling, seems to indicate that APMMA and SPMMA are essentially included between the crystalline PEO lamellae in both interlamellar and interphase zones, whereas IPMMA is present in the interfibrillar PEO spherulite regions. The presence of APMMA and SPMMA in the interlamellar regions and of IPMMA in the interfibrillar regions can also explain qualitatively the variation in the scattered intensity observed (see *Figure 4*). It is to be noted that no quantitative analysis on the absolute intensity has been performed on our samples. According to the statistical approach the scattering[35,44,45] is considered to arise from fluctuations in the electron density throughout the medium. The total scattering intensity is related directly to the mean square of the electron density fluctuation, $\overline{\eta^2}$, which for an ideal two-phase crystalline–amorphous system with sharp boundary is defined as

$$\overline{\eta^2} = (1-\phi_c) \times (\rho_c - \rho_a)^2 \qquad (12)$$

where ϕ_c is the volume crystallinity and ρ_c and ρ_a are the electron densities of the crystalline and amorphous phases, respectively.

As the values of the electron density of the amorphous PEO and APMMA are not different in a significant way[14,28], variations in the crystallinity will alter the values of $\overline{\eta^2}$ and cause the variation observed in the scattered intensity. In the case of PEO/IPMMA blends, assuming that the IPMMA is excluded from the regions between the lamellae, the scattering arises from a two-phase system consisting only of amorphous and crystalline lamellae of PEO. Consequently the slight decrease in the relative scattered intensity has to be attributed to increase in crystallinity of the PEO phase, observed by using d.s.c. measurements (see *Table 3*).

For the PEO/SPMMA and PEO/APMMA blends the two-phase system is formed, in our opinion, by PEO crystalline lamellae divided by amorphous layers containing PMMA and amorphous PEO. In this case, of course, the crystallinity of the two-phase system decreases with increase of PMMA, giving tise to the increase of $\overline{\eta^2}$.

If all the SPMMA and APMMA was in the interlamellar regions $(A+E)$, according to a two-phase model, the values of the long period of the PEO crystallized from PEO/APMMA and PEO/SPMMA blends, L_{cal}, could be estimated by the following relation, assuming volume additivity[26,30]:

$$L_{cal} = L_0 / V_2 \qquad (13)$$

where V_2 is the volume fraction of the crystallizable material in the blends and L_0 is the long period of the pure PEO obtained experimentally. The values of L_{cal}, calculated according to equation (13), are reported in *Table 6*. For the PEO/APMMA blend there is a quite good agreement between L_{cal} and the long period obtained experimentally, confirming that the APMMA is essentially included in interlamellar regions. In the case of PEO/SPMMA blends the L_{cal} values are surprisingly lower than the experimental ones, especially for blends at high SPMMA content. This result can be accounted for by assuming that interactions are present between the SPMMA and the PEO, in agreement with the decrease in the melting point observed for this system. In fact, interactions between molecules usually lead to changes in volume and hence no volume additivity can be assumed when we use equation (13).

CONCLUSIONS

The results of the investigation reported in the present paper have shown that PMMA tacticity strongly influences the miscibility of PEO/PMMA blends in the

Table 6 Comparison of the long period, calculated assuming all the PMMA to be in interlamellar regions, L_{cal}, with that obtained applying Bragg's law to the experimental data, L_{exp}

Blend composition, PEO/PMMA (wt/wt)	L_{cal} (Å)	L_{exp} (Å)	
		PEO/APMMA	PEO/SPMMA
100/0	270	270	270
90/10	301	285	340
80/20	338	291	340
70/30	378	338	600
60/40	451	500	720

melt. Consequently for a given crystallization condition the superstructure of the crystallized blends is influenced not only by composition but also by the configuration of PMMA used. SAXS and calorimetric analysis on PEO/PMMA blends seem to be consistent with the model of a pseudo-lamellar structure. In the case of PEO/APMMA and PEO/SPMMA the structure consists of PEO crystalline lamellae separated by amorphous and transition regions containing PEO and PMMA, whereas for the PEO/IPMMA system it consists of alternate crystalline and amorphous lamellae of PEO, with the IPMMA segregated in interfibrillar regions. These results, together with those concerning the analysis of T_g values, could indicate that in the range of composition and temperature studied, in the melt phase, the SPMMA is more miscible with the PEO than the IPMMA.

This conclusion seems to be in disagreement with the prediction made by Ramana Rao *et al.*[25], which indicated, as reported in the introduction, a preference of the PEO to form miscible blends with IPMMA instead of with SPMMA. In their calculation they consider for IPMMA and SPMMA a 3/1 helix and a planar zig-zag structure, respectively. As reported elsewhere by several authors[46-49], the conformation of lowest energy corresponds for IPMMA to a 10/1 helix having a pitch of 21.1 Å and for SPMMA, due to the difference between alternate backbone and bond angles, to a curved molecule with repeat distance of 5.7 Å. Considering the structures reported in the literature for the tactic forms of PMMA, we repeated the calculation in order to obtain more exactly the numbers of possible interaction sites for the PEO/PMMA blends. We have found, using the same approach followed by Ramana Rao *et al.*, that almost 50% of oxygen atoms of a PEO molecule can interact with the carbonyl carbon atom of a molecule of both IPMMA and SPMMA.

The calculation involved is based on the electronic charge distribution in the molecules and on the simultaneous occurrence of both negative and positive sites available for interaction. In order to interact, PEO has to act as a proton acceptor through the negative oxygen, whereas PMMA acts as a proton donor through the positive carbonyl carbon atom. It must be noted that in any case there cannot be a strong interaction between PEO and PMMA in PEO/PMMA blends, since the attractive forces between the negatively charged oxygen atoms of PEO and positively charged carbonyl carbon atoms of PMMA are weakened by the repulsive forces due to the two negatively charged oxygen atoms of PMMA. So on the basis of the atomic charge method, the total number and strength of the exchange interactions of PEO with IPMMA and SPMMA are almost the same and hence cannot explain the differences in phase behaviour observed experimentally for different blends. Neither can we invoke differences in molecular weight of the various PMMAs used, in order to justify the differences in miscibility of the three blends studied. In fact, IPMMA, having the lowest molecular weight (see *Table 1*), should be more compatible[6,7,10] with PEO than SPMMA and APMMA, contrary to what was found experimentally in this paper.

At this point we think we have to speculate on the difference in free-volume contribution and in particular on the difference in thermal expansivity between the various tactic forms of PMMA and PEO as responsible for the difference in mixing behaviour. As shown by MacMaster[10], the difference in thermal expansivity between two polymers is a very important factor in determining their mutual miscibility. In the case of PVC blends with PMMA having various configurations, such a difference seems to influence the miscibility as shown by a model calculation using Flory's equation-of-state theory[4].

Work is in progress along these lines in order to calculate the thermal expansion coefficient for SPMMA, IPMMA and PEO as a function of temperature and to verify our hypothesis.

ACKNOWLEDGEMENT

The authors would like to thank Mr Francesco Palumbo for his help in the preparation of all the figures of this paper.

REFERENCES

1 Schurer, J. W., de Boer, A. and Challa, G. *Polymer* 1975, **16**, 201
2 Roerdink, E. and Challa, G. *Polymer* 1980, **21**, 509
3 Roerdink, E. and Challa, G. *Polymer* 1978, **19**, 173
4 Vorenkamp, E. J., ten Brinke, G., Mejer, J. G., Jager, H. and Challa, G. *Polymer* 1985, **26**, 1725
5 Flory, P. J. 'Principles of Polymer Chemistry', Cornell University Press, Ithaca, NY, 1953
6 Olabisi, O., Robenson, L. M. and Shaw, M. T. 'Polymer–Polymer Miscibility', Academic Press, New York, 1979
7 Paul, D. R. and Newman, S. (Eds.) 'Polymer Blends', Academic Press, New York, 1978
8 Patterson, D. *Macromolecules* 1969, **2**, 674
9 Prigogine, I. 'The Molecular Theory of Solutions', North-Holland, Amsterdam, 1967
10 MacMaster, L. P. *Macromolecules* 1973, **6**, 760
11 Scott, R. L. and Hildebrand, J. L. 'The Solubility of Non-Electrolytes', Reinhold, New York, 1951
12 Patterson, D. *Polym. Eng. Sci.* 1982, **22**, 64
13 Nishi, T. and Wang, T. T. *Macromolecules* 1975, **8**, 909
14 Martuscelli, E., Silvestre, C., Addonizio, M. L. and Amelino, L. *Makromol. Chem.* 1986, **187**
15 Martuscelli, E., Pracella, M. and Yue, W. P. *Polymer* 1984, **25**, 1097
16 Martuscelli, E. and Demma, G. B. in 'Polymer Blends: Processing Morphology and Properties', (Eds. E. Martuscelli, R. Palumbo and M. Kryszewski), Plenum Press, New York, 1980
17 Martuscelli, E., Demma, G., Rossi, E. and Segre, A. L. *Polym. Commun.* 1983, **24**, 266
18 Martuscelli, E., Canetti, M., Vicini, L. and Seves, A. *Polymer* 1982, **23**, 331
19 Addonizio, M. L., Martuscelli, E. and Silvestre, C. *Polymer* in press
20 Hoffman, D. M. Ph.D. Thesis, University of Massachusetts, Amherst, 1979
21 Calahorra, E., Cortazar, M. and Guzman, G. M. *Polymer* 1984, **25**, 1097
22 Alfonso, G. C. and Russell, T. P. *Macromolecules* 1986, **19**, 1143
23 Cortazar, M. M., Calahorra, M. F. and Guzman, G. M. *Eur. Polym. J.* 1982, **18**, 165
24 Li, X. and Hsu, S. L. *J. Polym. Sci., Polym. Phys. Edn.* 1984, **22**, 1331
25 Ramana Rao, G., Castiglioni, C., Gussoni, M., Zerbi, G. and Martuscelli, E. *Polymer* 1985, **26**, 811
26 Liberman, S. A., Des Gomes, A. and Macchi, E. M. *J. Polym. Sci., Polym. Chem. Edn.* 1984, **22**, 2809
27 Silvestre, C., Karasz, F. E., MacKnight, W. J. and Martuscelli, E. in press
28 Stein, R. S. *et al. J. Polym. Sci., Polym. Symp.* 1978, **63**, 313
29 Kambatta, F. B. Ph.D. Thesis, University of Massachusetts, Amherst, 1976
30 Wenig, W., Karasz, F. E. and MacKnight, W. J. *J. Appl. Phys.* 1975, **46**, 4194
31 Morra, B. Ph.D. Thesis, University of Massachusetts, Amherst, 1980
32 Wai, M. P. Ph.D. Thesis, University of Massachusetts, Amherst, 1982

33 Vonk, C. G. *J. Appl. Crystallogr.* 1975, **8**, 340
34 Vonk, C. G. *J. Appl. Crystallogr.* 1973, **6**, 81
35 Alexander, L. E. 'X-Ray Diffraction in Polymer Science', Wiley, New York, 1969
36 Guinier, A. and Fournet, G. 'Small-Angle Scattering of X-Rays', Wiley, New York, 1955
37 Vonk, C. G. and Korleve, G. *Kolloid Z.Z. Polym.* 1967, **220**, 19; 1968, **224**, 125
38 Vonk, C. G. and Pijpers, A. P. *J. Polym. Sci., Polym. Phys. Edn.* 1985, **23**, 2517
39 Vidotto, G., Levy, D. L. and Kovacs, A. J. *Kolloid Z.Z. Polym.* 1968, **230**, 299
40 Rim, P. B. and Runt, J. P. *Macromolecules* 1981, **14**, 420
41 Rim, P. B. and Runt, J. P. *Macromolecules* 1984, **17**, 1520
42 Fox, T. G. *Bull. Am. Phys. Soc.* 1956, **2**, 123
43 Mandelkern, L. in 'Crystallization of Polymers', McGraw-Hill, New York, 1964
44 Debye, P. and Buche, A. M. *J. Appl. Phys.* 1944, **20**, 518
45 Stein, R. S. and Rowell, R. L. (Eds.) 'Electromagnetic Scattering', Gordon and Breach, New York, 1978
46 Tadokoro, H., Chatani, Y., Kusanagi, H. and Yokoyama, N. *Macromolecules* 1970, **3**, 441
47 Kusanagi, H., Tadokoro, H. and Chatani, Y. *Macromolecules* 1976, **3**, 531
48 Vacatello, M. and Flory, P. J. *Macromolecules* 1986, **19**, 405
49 Sudararajan, P. R. *Macromolecules* 1986, **19**, 415